

Chapter 6

Irradiating at RINSC

When irradiating at The State of Rhode Island Nuclear Science Center (RINSC), we have main methods at our disposal. Both have pros and cons associated with each one, which I will briefly describe below.

6.1 Rabbit Pneumatic Tube



Figure 6.1: Wooden "rabbit" stick with sensors attached,

Seen in figure 6.1 is a wooden stick with different sensors and attachments all held together with kapton tape. Directly in the center is a PSS halfmoon sensor which has already been initially measured, also on that same face are two PIN sensors. We use the PIN sensors for fluence estimations along each face (because there are slight

variations across a single face due to the orientation of the rabbit within the tube near the center of the reactor). In addition we also use the fluence values from each of the PIN diodes to better estimate the likely orientation of the rabbit stick during irradiation (which side was pointing up etc.). Orientation is important to us know because when the pneumatic tube is sent into the reactor, the spot where it rests during irradiation is orientated relative to the reactor core such that one side will be closer and occasionally one of the sides may be parallel to the flux of the neutrons.

One of the benefits of rabbit irradiation method over the beamport is that it allows for a shorter exposure time to the reactor, this is because once the time within the reactor is achieved the pneumatic tube can simply call the rabbit back where as in the beamport the process is more complex. A shorter time in the reactor allows greater consistency in fluences across different runs. Unfortunately though, due to the nature of how the rabbit stick is sent into the reactor it is not possible to precisely monitor the temperature within the rabbit stick. The only estimates of the temperature we are able to get are rough estimates on the maximum temperature with stickers we apply to the face of the rabbit. For this reason it is difficult to access the effect of concurrent annealing during irradiation which is important for longer irradiation (higher fluence) runs.

6.2 The Beam-Port

Some sensors needing to be irradiated are simply to big to put in a pneumatic tube, for this and other reasons the Brown Silicon Group also utilizes RINSC's beamport in addition to the rabbit tubes. The beamport is a large cylindrical hole which goes directly into the reactor (the aluminum vessel which houses the sensors and goes into the hole can be seen in figure 6.2 (c)). Currently we are using it to irradiate silicon sensors from the HGCAL group along with some test sensors used to monitor the fluence levels across runs. The test structures we are using to monitor the fluence in each run include the HGCAL and DZero cutouts. Additionally iron foils are placed with the sensors which we do isotope analysis on after to further determine what irradiation levels the sensors experienced.

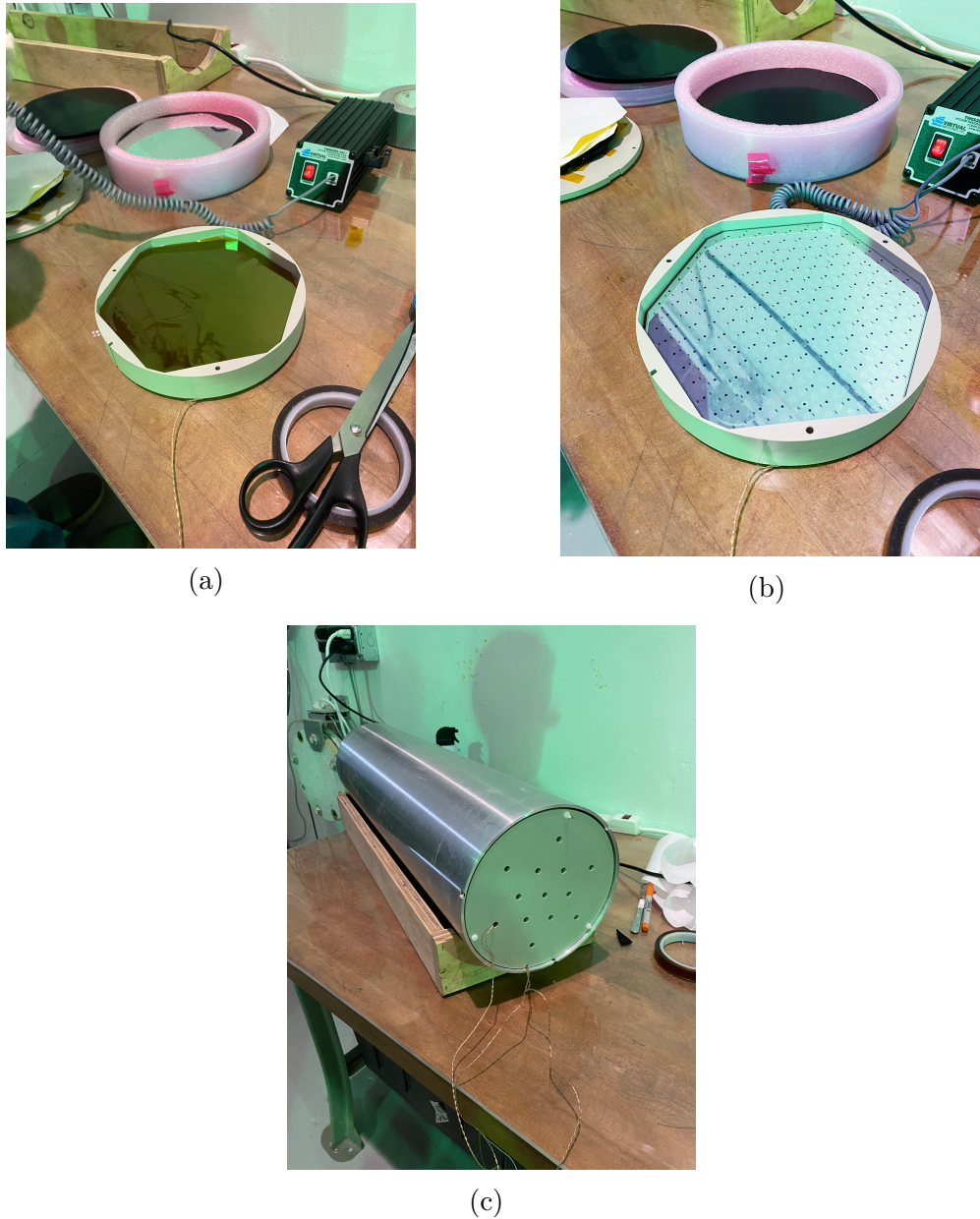


Figure 6.2: (a) Example of a kapton layer separating the different sensors of the beamport tube. (b) Hexagonal HGCAL sensor. (c) Beamport tube fully assembled with temperature sensor wires coming out.

The different sensors are "sandwiched" between layers of kapton film within the housing container (see figure 6.2 (a) and (b)). There are two primary layers, the front and the back, where naturally the front layer corresponds to the layer which is closest to the reactor core. Also included in each of the layers is a RTD (Resistance Temperature Detector) sensor which is able to record temperatures during irradiation in real time. What we have noticed during different irradiation runs is a

discrepancy between anticipated fluence and measured fluence, and also occasionally a significantly higher measured fluence for the sensors in the back of the beamport tube over the front of the tube. This of course should not be happening, due to the simple fact that the front of the beamport is closer to the neutron flux generated by the reactor core and therefore should ~~therefore~~ register a higher fluence. One of the clues for a possible cause is the temperature the sensors experience during irradiation.

Although the aluminum tube is filled with dry ice (solid CO_2), temperatures during irradiation can sometimes reach $+100^{\circ}C$ for extended periods of time. Of course the reactor core generates heat ~~and~~ so it is the front of the beamport that experiences a higher temperature. Our thinking is that there is a concurrent annealing effect occurring during irradiation which is leading to lower measured fluences. Analyzing these two concurrent effects on the HGCAL cutout silicon sensors will be the primary focus of the next chapter.

Chapter 7

Analysis

There are two main sections which comprise this chapter. The first section covers some PIN diode analysis which includes how one may use a PIN diode as a temperature sensor which is then used for the conversion formula between annealing PIN diodes at different temperatures. The second section involves the Hamburg model to infer the accumulated annealing of silicon sensors prior to their arrival at the Brown Silicon Lab. This analysis was used when doing a calibration check between two different CMS irradiation sites; Ljubljana and RINSC (the irradiation site the Brown Silicon group uses). The other part of the Hamburg analysis included in this chapter is the analysis of the concurrent annealing and irradiation effect on the beampart HGCAL cutout silicon sensors.

7.1 PIN Analysis

As mentioned above, this section outlines an analysis of the effect of temperature on unirradiated PIN diodes which was then used to inform us on how best to do an annealing study for PIN diodes. The main question in the temperature study was: "if we place a PIN diode inside of an oven set at a specific temperature, how long does it take for that PIN diode to saturate to that temperature?". We then used the answer from that question to better access how much annealing occurred in one annealing step. We then took that to then find how the effect of annealing on irradiated PIN diodes scale with temperature, and whether that effect scaled exponentially like was found previously for other silicon sensors.

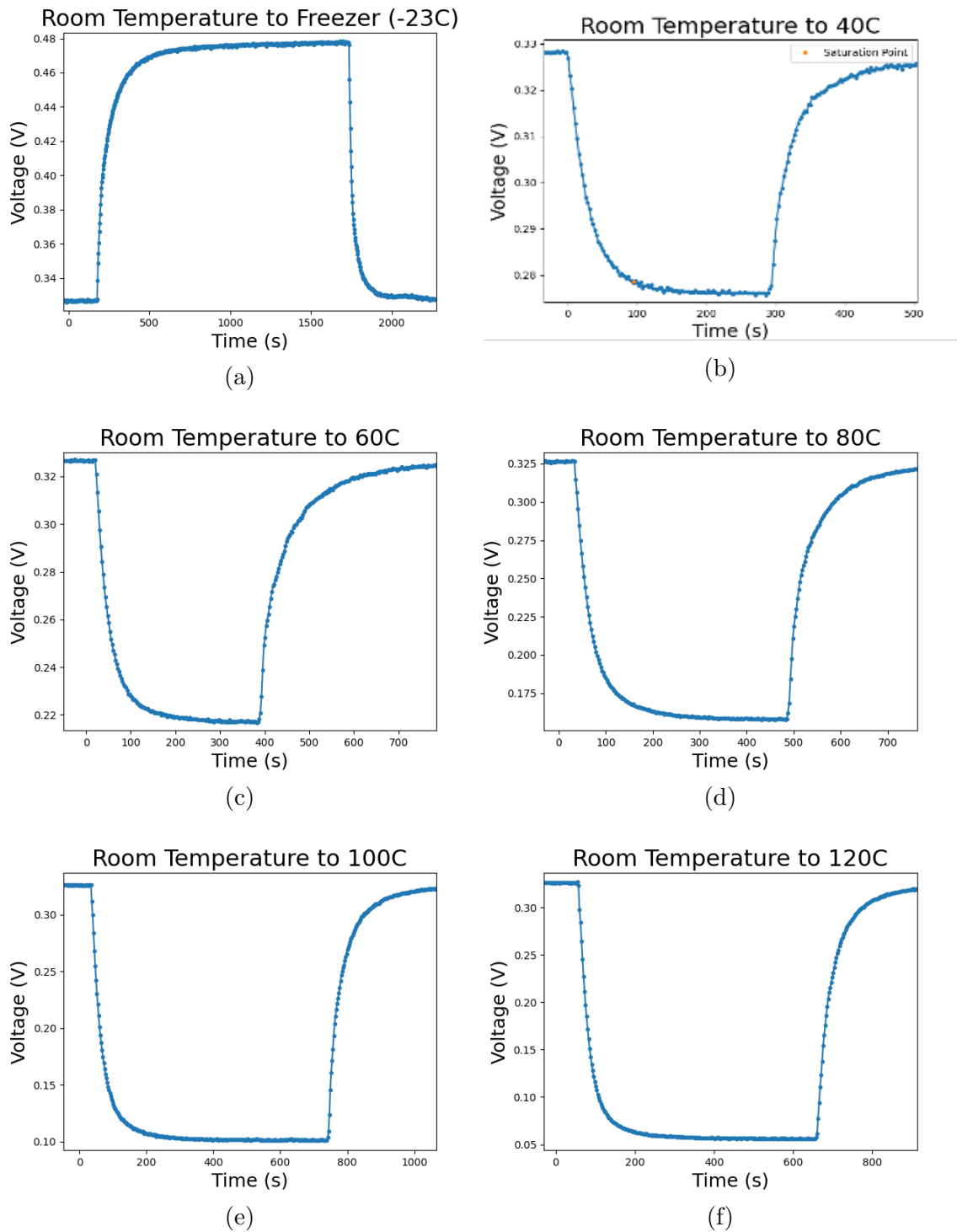


Figure 7.1: Forward voltage (V_f) vs. time for an unirradiated PIN diode

7.1.1 Temperature Study

The method we used for determining the effect of temperature on unirradiated PIN diodes was to measure every second the forward voltage (V_f) response of applying a

$1mA$ pulse for $12mS$. What we found (shown in figure 7.1) was that if we define the saturation forward voltage (V_{sat}) as the value of the forward voltage after prolonged exposure to a specific temperature, then the saturation voltage vs. temperature follows a linear relationship for values of temperature $T \in (-20^{\circ}C, 100^{\circ}C)$.

This result can be seen in figure 7.2, while this was interesting we did not pursue this any further. Instead we changed the method with which we were heating up the PIN diodes within the oven so that the ramp up time plus the ramp down time was less than 1% of the total annealing time. This was important because the value we were interested in, with regard to the PIN diodes, was the ~~affect~~ of cumulative annealing. So ensuring that time quoted at a specific temperature was in fact that time was important. We achieved this by changing annealing from an aluminum tray to a thick aluminum plate which was always within the oven. This ensured that there would be more effective thermal contact which reduced the ramp up time. Once annealed we then placed the PIN diodes onto another aluminum plate at room temperature, we found that by doing this our ramp up and ramp down times would be less than 1% of the annealing time if the annealing steps were greater than 10 minutes.

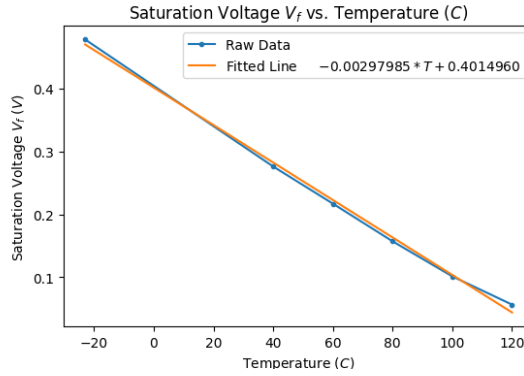


Figure 7.2: Result of PIN-thermometer analysis, found that ramp-up-time would significantly affect cumulative annealing time for short-duration annealing if Annealed on surface not already pre-heated to oven temperature.

7.1.2 Annealing Study

The PIN annealing study, as briefly described above, was intended to answer the question ~~of~~ is there a way to convert between different annealing temperatures in a

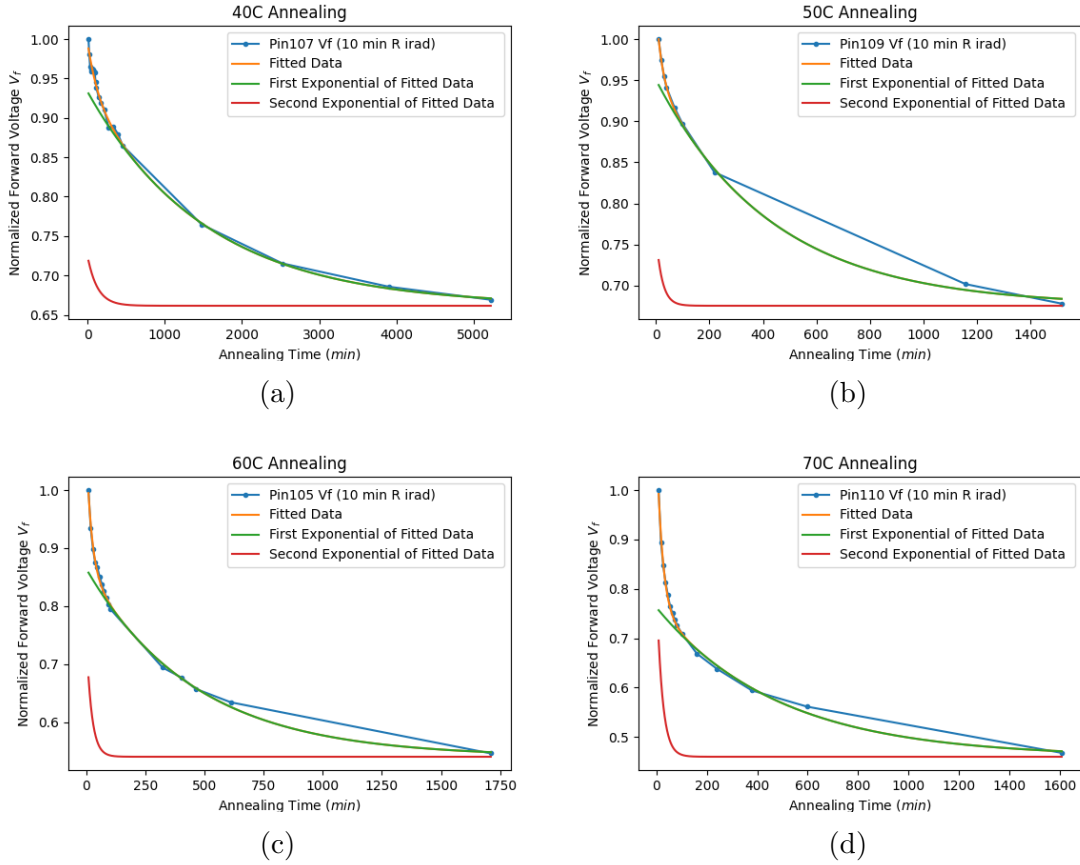


Figure 7.3: Normalized forward voltage (V_f) vs. cumulative annealing time for PIN-diodes for 40°C , 50°C , 60°C and 70°C

simple way. This was relevant to our group because we were curious if there was a way to account for annealing in the way we accounted for annealing for other diodes we worked with. In particular we were interested in being able to integrate over the temperatures experienced by the diode in question in order to come up with a number which we could use to understand the cumulative annealing in a simple way. Getting the data was a simple but time consuming process. The PIN diodes used in this analysis were all from the same rabbit irradiation run. The irradiation run was also very short at 10 minutes, we decided to use PIN diodes from such a run because we found that concurrent annealing and irradiation ~~affects~~ were minimized for low fluences. Annealing temperatures were chosen based on the temperatures sensors experienced in the rabbit (since we only use the PIN diodes in the rabbit) and at the time our temperature stickers were indicating that the maximum temperature experienced was 70°C . The results of the analysis and can be seen in figure 7.3 and

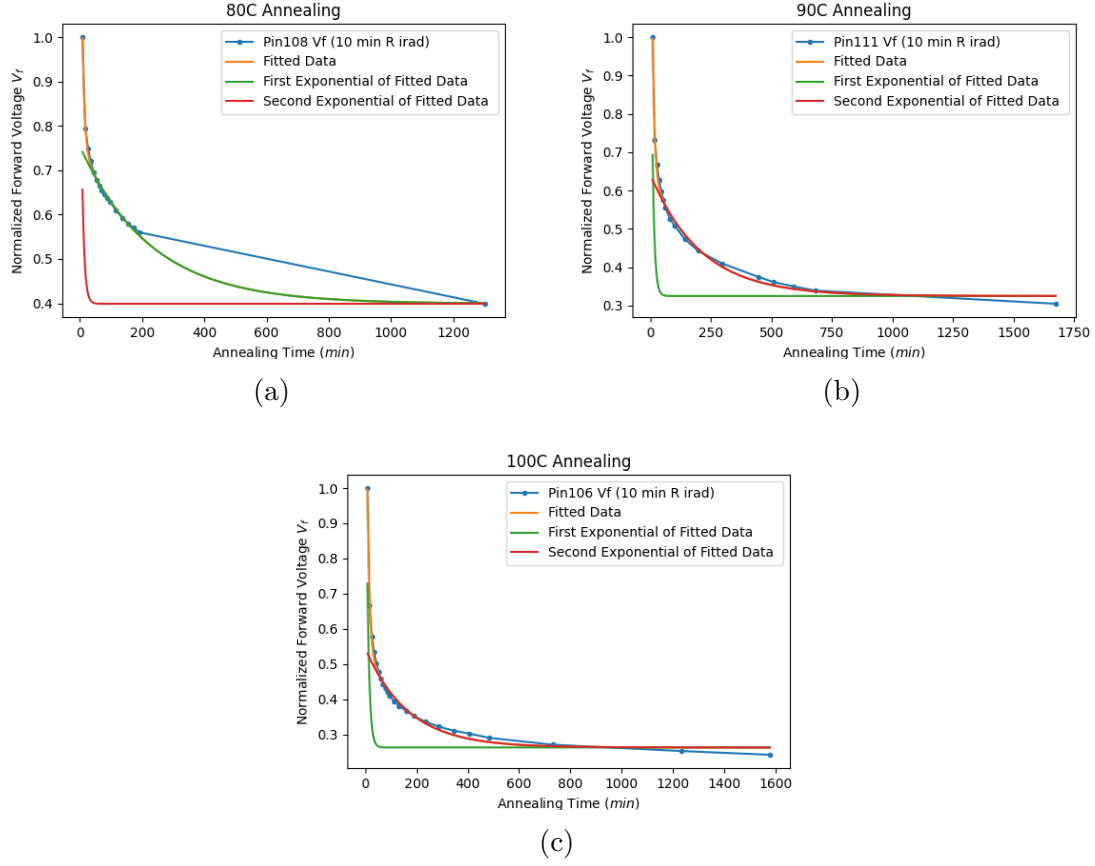


Figure 7.4: Normalized forward voltage (V_f) vs. cumulative annealing time for PIN-diodes for $80^{\circ}C$, $90^{\circ}C$ and $100^{\circ}C$

[7.4](#), in these graphs we normalized to the initial forward voltage of the PIN diode without any annealing. We decided to fit the data to a sum of two exponential of the form:

$$f(x) = a \cdot e^{b \cdot t} + c \cdot e^{d \cdot t} \quad (7.1)$$

where a, b, c and d are all free parameters, we did this for each of the annealing temperatures. Then, to be able to compare the temperatures to one another, we decided to compare the annealing temperature which had the most robust data to the others. This turned out to be the $100^{\circ}C$ data, and the form of the function we used to match the others was the following.

$$f_{100^{\circ}C}(x) \rightarrow f(a(t - b)) \quad (7.2)$$

the intuition behind the two parameters is that “a” accounts for the strength of the annealing (assuming an exponential response in temperature) while “b” accounts for

any pre-annealing that occurred in the reactor. The results of the parameter fitting is summarized in the table 7.1

Annealing Temperature	a [$\frac{1}{t}$]	b [t]
40°C	1.88e-03	-2.018e+03
50°C	7.19e-03	-4.58e+02
60°C	1.40e-02	-3.37e+02
70°C	3.08e-02	-1.68e+02
80°C	0.11	-32.50
90°C	0.28	-10.44
100°C	1.06	7.14

Table 7.1: Annealing Fitting Parameters

The result of plotting the exponential scale factor (a) to annealing temperature can be seen in figure 7.5, where indeed we see an exponential relationship between that scale factor and the different annealing temperatures. The function which was fitted to the data was the same as that which we used for D0 diodes, with this function we can now (listed in the legend of 7.5) compare annealing temperatures to themselves and then use that information to estimate the fluence when the diode came first out of the reactor.

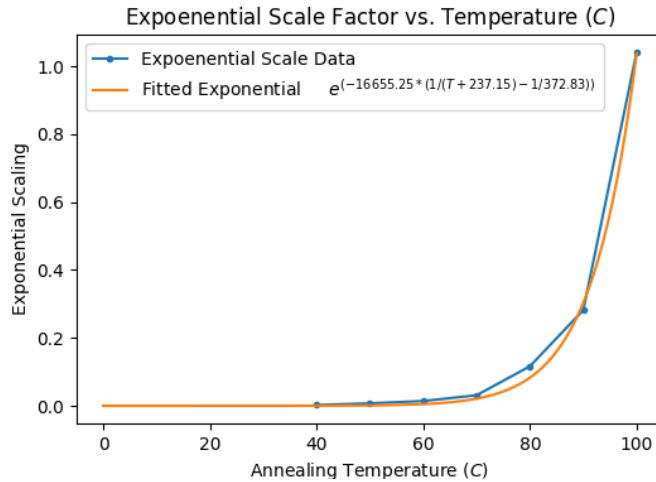


Figure 7.5: Exponential scale factor vs. temperature for PIN diodes

7.2 Hamburg Model Analysis

This section deals with two instances where we annealed irradiated diodes and then used the Hamburg Model on that data to infer information about the annealing which either occurred during transportation to the Brown Silicon Lab or annealing which occurred during the irradiation process. The first part of this analysis will speak about the use of the Hamburg Model on diodes which we suspected were annealed on transit to our lab. The second part will consider the effects of concurrent annealing and irradiation effects, this is of concern for the Brown Silicon Group and the HGCAL group because we both analyze properties of silicon sensors irradiated in the beamport at RINSC. This particular irradiation location experiences high temperatures throughout irradiation even when precautions are made (like filling the tube with dry ice), so better understanding how these effects are combined is critical to continued use of the beamport at RINSC and which may further lead to improvements on how those sensors are irradiated or greater understanding on the play between concurrent irradiation and annealing.

7.2.1 Ljubljana Diodes

Two of the main irradiation locations for the CMS group are RINSC and Ljubljana, for that reason there was an effort made to cross calibrate these two locations quoted fluences in order to have greater consistency within the collaboration. During this cross calibration check there were PIN and DZero diodes sent to Ljubljana irradiated at four separate fluences ($6.5e14$, $1.5e15$, $2.5e15$ and $5e15 \text{ MeVn/cm}^{-2}$) and we were to measure those diodes using our lab equipment to see how well our values lined up with what Ljubljana quoted they should be. Initially there was discrepancy between the two values, and so the Brown Silicon group looked to see what might be the cause. There were a few candidates for what might be reason for this discrepancy, those ideas were:

1. Our volume measurement for D0 diode are not accurate
2. Diodes over irradiated, therefore results not accurate

- Annealing occurred during transportation to Brown, which caused lower fluence measurements

The first point was looked into, and we then found that the depth value we were using for the diode was off, which did lead to an improvement (to be discussed in section 8.1). The second point was immediately apparent, for only the $6.5e14 \text{ MeVn/cm}^{-2}$ diodes were depleting below our maximum voltage of 1100V's. Therefore, our estimates for those higher fluence values could only be interpreted as lower bounds. Then, given that the transportation box (which originally had dry ice inside) did not contain dry ice, we decided to pursue the third point.

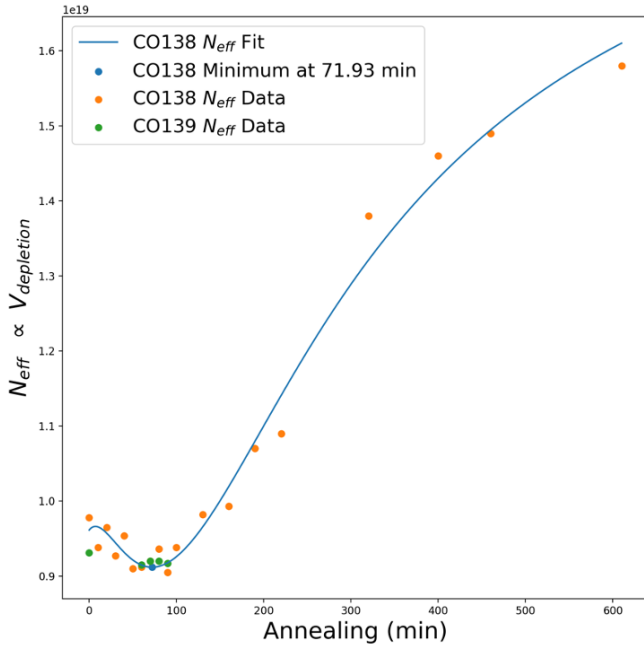


Figure 7.6: Ljubljana Hamburg analysis of DZero diodes to determine possible transportation annealing en route to Brown University from Slovenia

Unfortunately there was no remote temperature sensor within the transportation box so we only had rough estimates of what the temperature likely was. For this reason we resorted to the Hamburg model to see if we could estimate what annealing occurred based on the minimum of the N_{eff} vs. Annealing Time graph. For D0's we have measured in the past in our own lab, and D0's similarly measured and analyzed at Fermilab, we expect a minimum in that data to occur at 80 minutes of annealing

at $60^{\circ}C$ - any deviation from that would indicate annealing during transportation to Brown.

We decided to anneal a D0 diodes from the $6.5e14 \text{ MeVn/cm}^{-2}$ batch at 10 minute increments up to 100 minutes, and then open up the step sizes once a lot of the subtle changes in N_{eff} subsided. The depletion voltage was measured for each of these annealing steps, and the results were fed into equation 3.5 to arrive at figure 7.6. Based on the minimum of the Hamburg fit occurring at 71.93 minutes, we can be reasonable sure that approximately 8 minutes of annealing occurred on the trip from Slovenia to Providence, Rhode Island. When converting between annealing temperatures, we find that 8 minutes of annealing at $60^{\circ}C$ is equivalent to 33 hours at $20^{\circ}C$ - a reasonable estimate for the length of travel time without dry ice. These results are interpreted into the general results of the RINSC-Ljubljana/JSI cross calibration in section 8.1.

7.2.2 HGCAL Diodes

This section, as mentioned earlier, will cover the Hamburg Model analysis results on the HGCAL cutout diodes which were irradiated in the beampipe at the RINSC irradiation facility. Within the different irradiation runs were also some D0 diodes (largely ineffective at giving reliable fluence estimates for irradiation times greater than 25 minutes due to the depletion voltage being greater than the 1100V limit), iron foils and full scale HGCAL hexagonal silicon diodes. Photos of this arrangement can be found in section 6.2. The objective of this analysis was to try and shine a light on the interplay between annealing and irradiation during irradiation. Some of the HGCAL rounds experienced as much as 10,000 minutes of equivalent annealing at $60^{\circ}C$ which would of course affect the resulting measured fluence. The following grouping of plots constitute seven different irradiation runs, each of the runs will be briefly described before a full analysis of the results is discussed in section 8.2.

For the following analysis I will think of N_{eff} as a function of annealing time $N_{eff}(t)$, where $t_{min}^{60^{\circ}C}$ is the cumulative annealing at $60^{\circ}C$ which resulted in a minimum in $N_{eff}(t)$. Also, $\Phi_{eq}(t_{min}^{60^{\circ}C})$ is the fluence value which is extracted when using the

data from the minimum of the $N_{eff}(t)$ curve. Finally, I will define A_{60^oC} as the cumulative equivalent annealing at 60^oC .

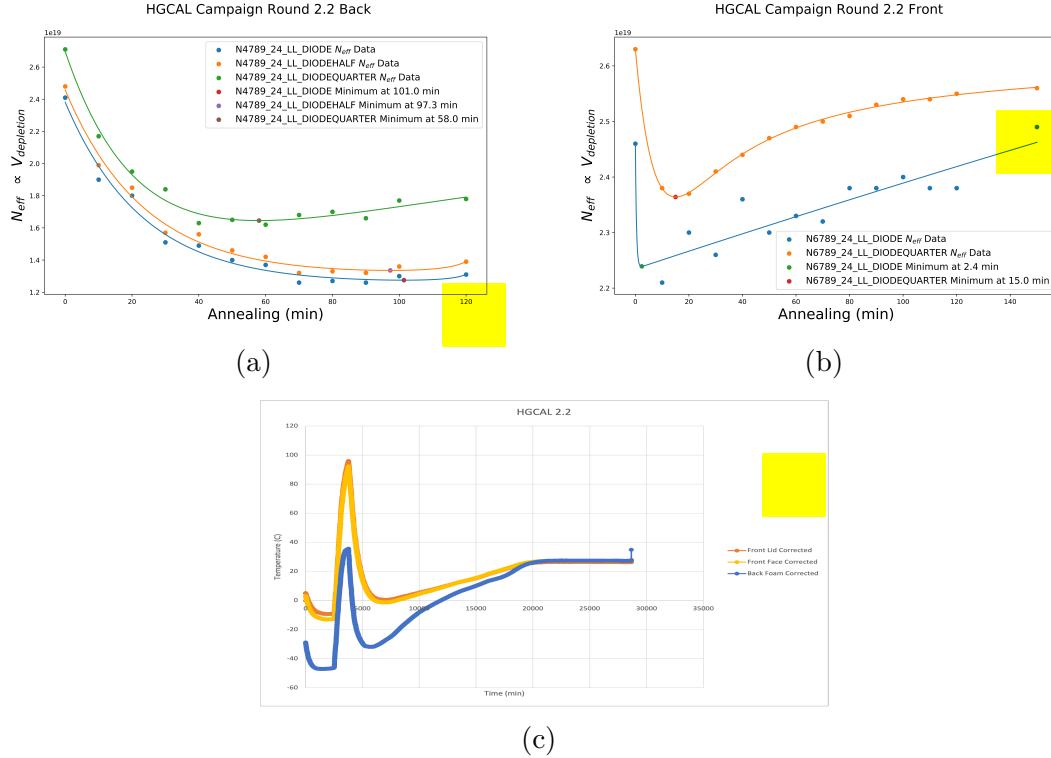


Figure 7.7: Hamburg analysis of HGCAL diodes irradiated at RINSC for 43 minutes. (a) HGCAL diode at back of beamport, (b) HGCAL diode at front of beamport, (c) temperature profile from start of irradiation to them being pulled out.

In HGCAL round 2.2 (figure 7.7) we can notice that the front diode experienced a higher temperature with a cumulative equivalent annealing at 60^oC of 504 minutes whereas the back diode experienced approximately 6.01 minutes of cumulative equivalent annealing at 60^oC .

Diode	Location	$t_{min}^{60^oC}$	$\Phi_{eq}(t_{min}^{60^oC})$	A_{60^oC}
DIODE	BP Front	15.0	9.54E+14	504
DIODEQUARTER	BP Front	2.4	1.08E+15	504
DIODE	BP Back	101.0	1.35E+15	6.01
DIODEHALF	BP Back	97.3	1.28E+15	6.01
DIODEQUARTER	BP Back	58.0	1.61E+15	6.01

Table 7.2: HGCAL Round 2.2 Extracted Hamburg Values

Therefore we expect the minimum of N_{eff} to occur at a lower cumulative annealing for the front diodes, this is in-fact the case and we can see that the DIODE

for the front HGCAL cutout saw a minimum occur at 15.0 minutes where DIODE on the back HGCAL cutout had a minimum at 101.0. Although we expect a higher measured fluence for the cutout on the front of the beamport, the opposite is the case. From table 7.2 we can see that the fluence estimate is nearly 30% higher for the back DIODE than for the front.

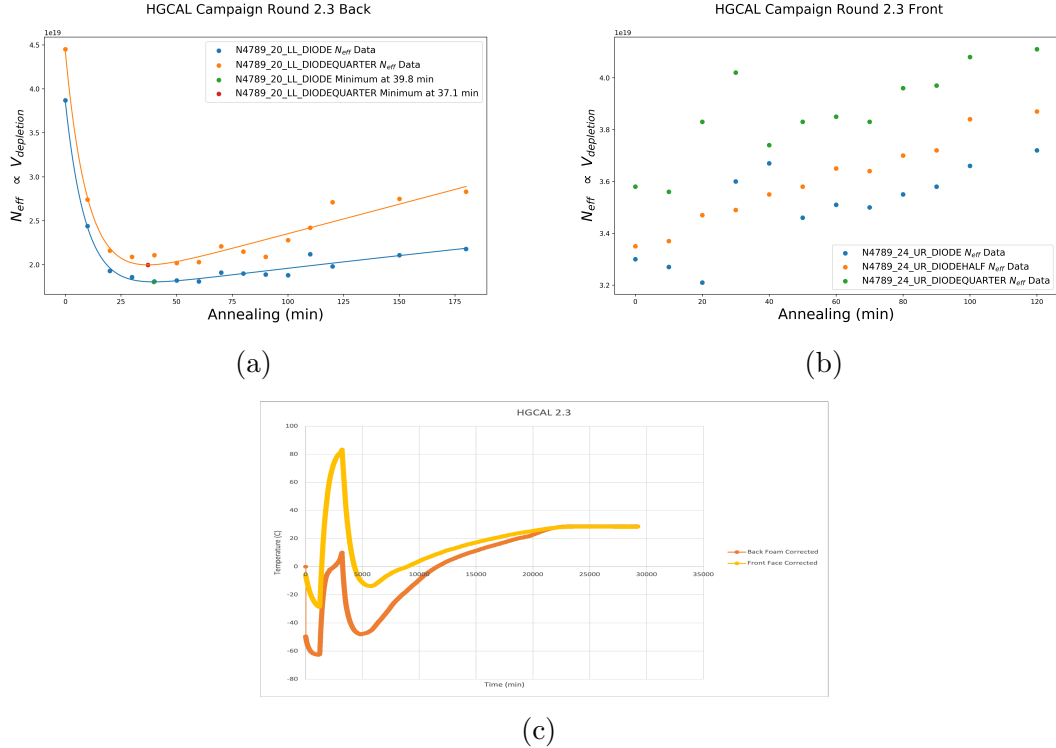


Figure 7.8: Hamburg analysis of HGCAL diodes irradiated at RINSC for 86 minutes

In HGCAL round 2.3 (seen in figure 7.8) we can see a very close agreement between the two diodes on the BP_Back HGCAL cutout while the BP_Front diodes seem to have experienced so much annealing during irradiation that they ~~past~~ the minimum ($N_{eff}(t_{min}^{60^{\circ}C})$) prior to being brought back from RINSC.

Diode	Location	$t_{min}^{60^{\circ}C}$	$\Phi_{eq}(t_{min}^{60^{\circ}C})$	$A_{60^{\circ}C}$
DIODE	BP Front	0	2.08E+15	374
DIODEHALF	BP Front	0	2.15E+15	374
DIODEQUARTER	BP Front	0	2.35E+15	374
DIODE	BP Back	39.8	2.78E+15	5.62
DIODEQUARTER	BP Back	37.1	3.09E+15	5.62

Table 7.3: HGCAL Round 2.3 Extracted Hamburg Values

This is confirmed by the data in table 7.3 which indicates the front diodes

experienced 374 minutes of cumulative annealing at $60^{\circ}C$ to the back diodes 5.62 minutes. Although the cumulative annealing analysis would seem to indicate that $N_{eff}(t_{min}^{60^{\circ}C})$ should occur at ~ 70 minutes, we instead find that it occurs at ~ 40 minutes. The fluence estimates for this round were again flipped from what we would have expected them to be, with the front DIODE measuring $2.08 \cdot 10^{15} \text{ MeVn/cm}^{-2}$ to the back DIODE's $2.78 \cdot 10^{15} \text{ MeVn/cm}^{-2}$, a 33% difference between the two.

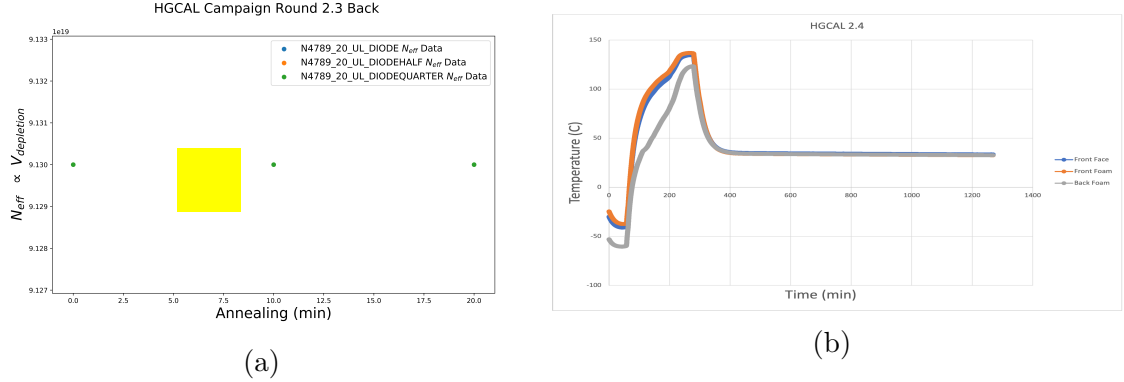


Figure 7.9: Hamburg analysis of HGCAL diodes irradiated at RINSC for 216 minutes

HGCAL round 2.4 was irradiated for significantly longer than any of the other rounds, and due to the prolonged exposure to the reactor core (216 minutes) there was a few unintended consequences. The plastic bags that we put the diodes into shrunk in the heat, and the bag for the front diode snapped in half as a result of that shrinking. Although the temperature sensors and HGCAL cutout from the back of the beamport did survive the extended exposure.

Diode	Location	$t_{min}^{60^{\circ}C}$	$\Phi_{eq}(t_{min}^{60^{\circ}C})$	$A_{60^{\circ}C}$
DIODE (Destroyed)	BP Front	NA	NA	106,709
DIODEHALF(Destroyed)	BP Front	NA	NA	106,709
DIODEQUARTER (Destroyed)	BP Front	NA	NA	106,709
DIODE	BP Back	0	1.84E+16	27,252
DIODEHALF	BP Back	0	1.58E+16	27,252
DIODEQUARTER	BP Back	0	1.67E+16	27,252

Table 7.4: HGCAL Round 2.4 Extracted Hamburg Values

In figure 7.9 we can see the results of the extended exposure, the back of the beamport received a cumulative equivalent annealing of 27,252 minutes. We were not able to identify a depletion voltage on the probe station, and so our estimates for the fluence in table 7.4 should be viewed as a lower-bound only.

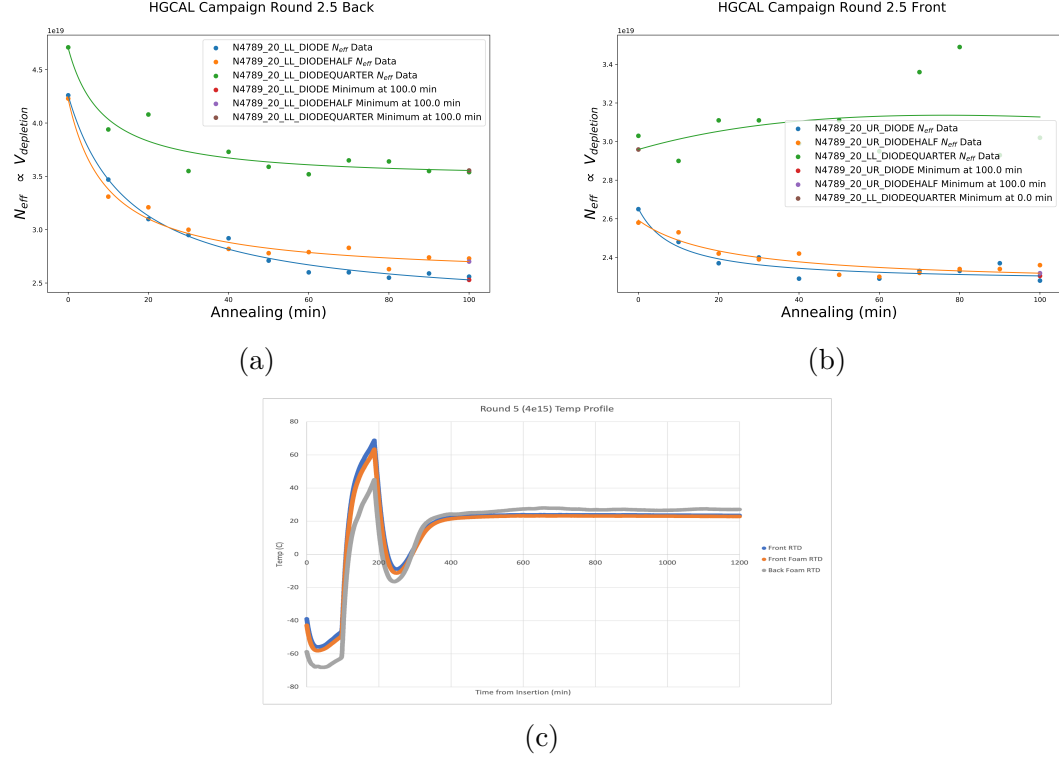


Figure 7.10: Hamburg analysis of HGCAL diodes irradiated at RINSC for 86 minutes

HGCAL round 2.5 was irradiated for 86 minutes, and although the diodes on the front and back experienced very different cumulative equivalent annealing (69.17 minutes for the front and 11 minutes for the back) their N_{eff} vs. Annealing graphs showed very similar results.

Diode	Location	$t_{min}^{60^{\circ}C}$	$\Phi_{eq}(t_{min}^{60^{\circ}C})$	$A_{60^{\circ}C}$
DIODE	BP Front	100.0	2.81E+15	69.17
DIODEHALF	BP Front	100.0	2.90E+15	69.17
DIODEQUARTER	BP Front	NA	3.31E+15	69.17
DIODE	BP Back	100.0	2.35E+15	11
DIODEHALF	BP Back	100.0	2.93E+15	11
DIODEQUARTER	BP Back	100.0	3.35E+15	11

Table 7.5: HGCAL Round 2.5 Extracted Hamburg Values

In table 7.5 we can see that the fluence value for the front DIODE was in fact higher than the back, which is what we expect should happen. Its not quite clear what happened in BP_Front DIODEQUARTER, though since this is the smallest diode it is not cause for concern and should be dismissed.

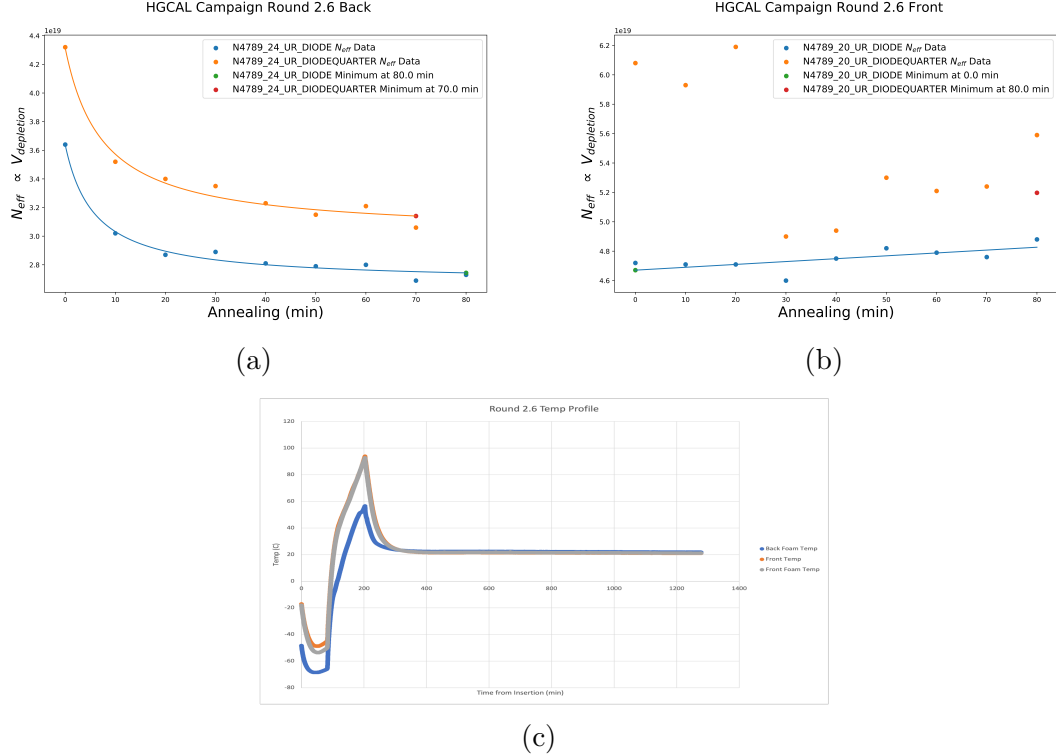


Figure 7.11: Hamburg analysis of HGCAL diodes irradiated at RINSC for 118 minutes

HGCAL round 2.6 was another one of the longer irradiation runs at 118 minutes, and we can see the effects of the longer irradiation in the front HGCAL cutout.

Diode	Location	$t_{min}^{60^{\circ}C}$	$\Phi_{eq}(t_{min}^{60^{\circ}C})$	$A_{60^{\circ}C}$
DIODE	BP Front	0	2.86E+15	739.3
DIODEQUARTER	BP Front	0	3.35E+15	739.3
DIODE	BP Back	80.0	3.68E+15	20.6
DIODEQUARTER	BP Back	70.0	4.16E+15	20.6

Table 7.6: HGCAL Round 2.6 Extracted Hamburg Values

In table 7.6 we can see what is partially reflected in figure 7.11, that a cumulative equivalent annealing of 739.3 minutes was more than significant enough to push N_{eff} into the region where each successive annealing step resulted in a higher N_{eff} . Looking at the diodes in the back of the beamport we register a cumulative equivalent annealing of 20.6 minutes and so suspect a minimum to occur at around 60 minutes. Further measurements need to be taken in order to better understand the overall curve.

In the above figures 7.12 we can see the results of the Hamburg analysis for

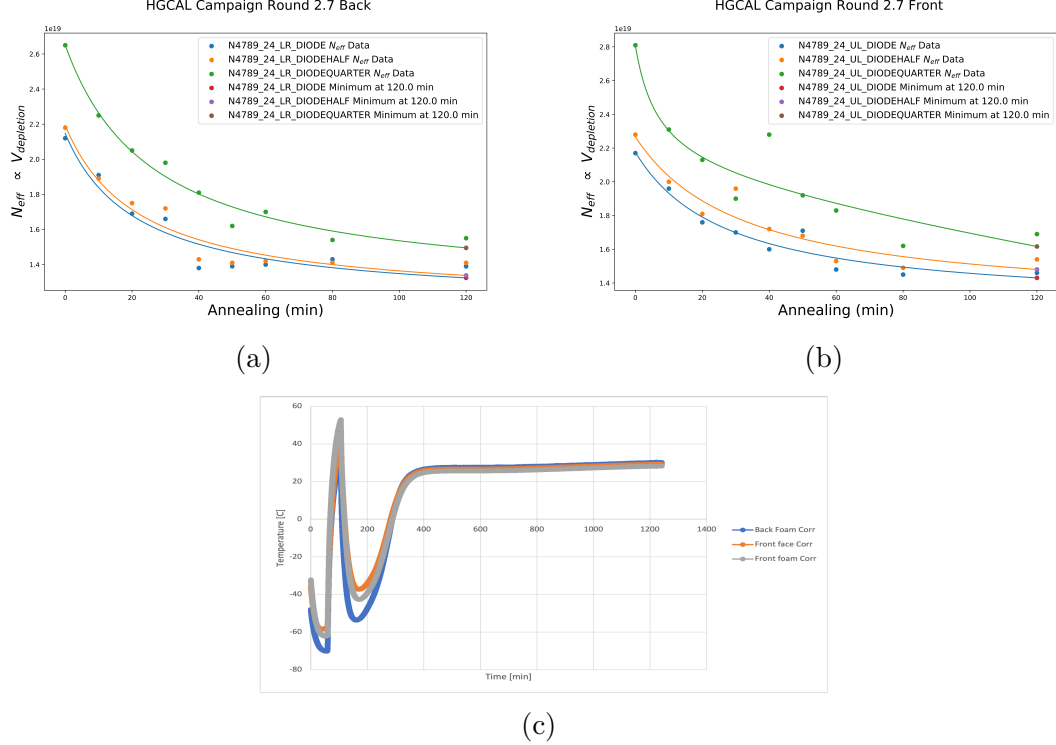


Figure 7.12: Hamburg analysis of HGCAL diodes irradiated at RINSC for 43 minutes

HCGAL 2.7, a shorter irradiation run at 43 minutes. The Hamburg fit for both of the data seem to have missing an apparent minimum at 80 minutes for the both, so this is the value I have manually entered into the table below. Additional measurement steps would have helped flush out the detail in the minimum region, future diode measurement staff in the Brown Silicon lab could consider taking this a bit further to better understand this particular run.

Diode	Location	$t_{min}^{60^{\circ}C}$	$\Phi_{eq}(t_{min}^{60^{\circ}C})$	$A_{60^{\circ}C}$
DIODE	BP Front	80.0	1.51E+15	12.6
DIODEHALF	BP Front	80.0	1.57E+15	12.6
DIODEQUARTER	BP Front	80.0	1.70E+15	12.6
DIODE	BP Back	80.0	1.27E+15	13.09
DIODEHALF	BP Back	80.0	1.40E+15	13.09
DIODEQUARTER	BP Back	80.0	1.53E+15	13.09

Table 7.7: HGCAL Round 2.7 Extracted Hamburg Values

In table 7.7 we can see that once again the front diode measured a higher fluence than the back diodes, and they both experienced very similar cumulative equivalent annealing at 12.6 minutes for the front cutout and 13.09 for the back. It does look

like with further measurements more could be said, if I had more time to measure this in my mind would be the run to do.

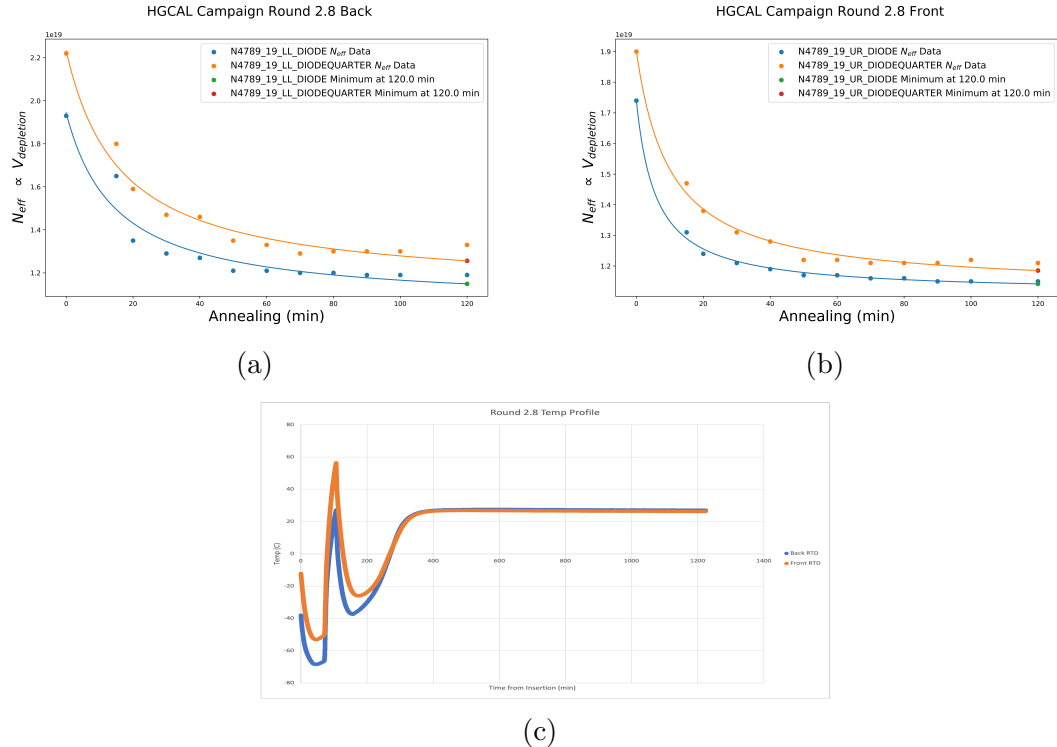


Figure 7.13: Hamburg analysis of HGCAL diodes irradiated at RINSC for 32 minutes

The final HGCAL round I will be discussing in 2.8, this round was irradiated for 43 minutes and the Hamburg fit for these diodes were especially well behaved. Again, it does look like from the data that the minimum occurs in the region of 80 minutes, although due to there not being more data for higher annealing values the fitting of the Hamburg model to the data did not adequately pick up on this minimum region.

Diode	Location	$t_{min}^{60^{\circ}C}$	$\Phi_{eq}(t_{min}^{60^{\circ}C})$	$A_{60^{\circ}C}$
DIODE	BP Front	80.0	1.06E+15	14.4
DIODEQUARTER	BP Front	80.0	1.18E+15	14.4
DIODE	BP Back	80.0	1.05E+15	10.9
DIODEQUARTER	BP Back	70.0	1.11E+15	10.9

Table 7.8: HGCAL Round 2.8 Extracted Hamburg Values

In table 7.8 we can see again that the equivalent cumulative annealing were very similar for both the front and back diodes, at 14.4 minutes for the front and 10.9 minutes for the back. Additionally the fluence measurements were very closer for

both of the larger diodes with the front DIODE measuring $1.06 \cdot 10^{15} \text{ MeVn/cm}^{-2}$ to the back DIODE's $1.05 \cdot 10^{15} \text{ MeVn/cm}^{-2}$.

Chapter 8

Conclusions

The following two sections conclude this thesis, the first section will serve to finalize the JSI/Ljubljana-RINSC cross calibration analysis. The second section will summarize the data gathered on the Hamburg analysis of seven irradiation runs. Finally a discussion on possible future directions, primarily with respect to the question of the effect of concurrent annealing and irradiation on silicon sensors, will close this paper.

8.1 RINSC-Ljubljana Cross Calibration

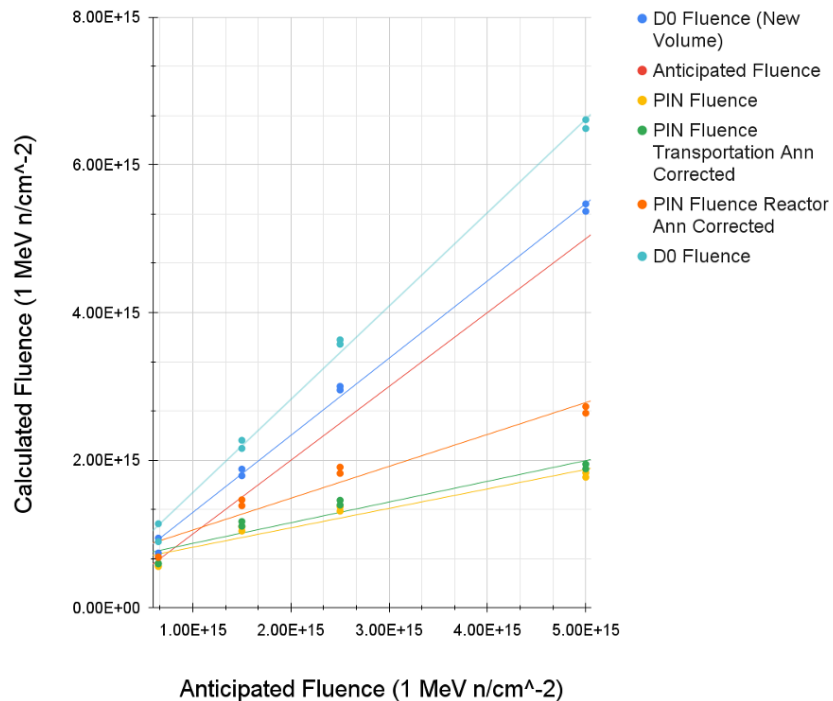


Figure 8.1: Calculated fluence of PIN and D0 diodes vs. Ljubljana anticipated values

In figure 8.1 we can see the initial D0 fluence estimate in light blue, which is far

above the estimate given to us by Ljubjana. From here we investigated further and found that our value for the volume of the diode was off which lead to our fluence estimate for the D0 diodes indicated by the blue line. This we found to be within the error and so felt we had achieved agreement with the fluence results of Ljubjana.

8.2 Effects of Concurrent Annealing and Irradiation

8.3 Future Work

Bibliography

- [1] W. Adam et al. ‘P-Type Silicon Strip Sensors for the new CMS Tracker at HL-LHC’. In: *Journal of Instrumentation* 12.06 (June 2017), P06018–P06018. doi: [10.1088/1748-0221/12/06/p06018](https://doi.org/10.1088/1748-0221/12/06/p06018). URL: <https://doi.org/10.1088/1748-0221/12/06/p06018>.
- [2] Adundovi. *A P-N Junction in Thermal Equilibrium*. URL: https://en.wikipedia.org/wiki/P%2880%93n_junction.
- [3] Alexander Furgeri. ‘Quality assurance and irradiation studies on CMS silicon strip sensors’. PhD thesis. Karlsruhe U., 2006.
- [4] Julie Haffner. ‘The CERN accelerator complex. Complexe des accélérateurs du CERN’. In: (Oct. 2013). General Photo. URL: <https://cds.cern.ch/record/1621894>.
- [5] M.R. Hoeferkamp et al. ‘Application of p–i–n photodiodes to charged particle fluence measurements beyond 10^{15} 1-MeV-neutron-equivalent/cm²’. In: *Nuclear Instruments and Methods in Physics Research Section A: Accelerators, Spectrometers, Detectors and Associated Equipment* 890 (2018), pp. 108–111. ISSN: 0168-9002. doi: <https://doi.org/10.1016/j.nima.2018.02.070>. URL: <https://www.sciencedirect.com/science/article/pii/S0168900218302249>.
- [6] Gerhard Lutz. *Semiconductor Radiation Detectors*. Berlin: Springer, 1999. URL: <https://cds.cern.ch/record/887388>.
- [7] Ricardo Marco-Hernandez. ‘A Portable Readout System for Microstrip Silicon Sensors (ALIBAVA)’. In: *IEEE Transactions on Nuclear Science* 56.3 (2009), pp. 1642–1649. doi: [10.1109/TNS.2009.2017261](https://doi.org/10.1109/TNS.2009.2017261).
- [8] Marius Metzler. ‘Irradiation studies on n-in-p silicon strip sensors in the course of the CMS Phase-2 Outer Tracker Upgrade’. PhD thesis. Karlsruhe Institute of Technology (KIT), 2020.

- [9] Michael Moll. ‘Displacement Damage in Silicon Detectors for High Energy Physics’. In: *IEEE Transactions on Nuclear Science* 65.8 (2018), pp. 1561–1582. DOI: [10.1109/TNS.2018.2819506](https://doi.org/10.1109/TNS.2018.2819506).
- [10] Michael Moll. ‘Radiation damage in silicon particle detectors: Microscopic defects and macroscopic properties’. PhD thesis. Hamburg U., 1999.
- [11] Jason Röhr. ‘Electron Transport in Solution Processed Antimony Sulphide Thin Films made from a Xanthate Precursor’. PhD thesis. Sept. 2014. DOI: [10.13140/RG.2.2.29530.39366](https://doi.org/10.13140/RG.2.2.29530.39366).
- [12] Leonardo Rossi et al. *Pixel detectors: from fundamentals to applications*. Particle acceleration and detection. Berlin: Springer, 2006. DOI: [10.1007/3-540-28333-1](https://doi.org/10.1007/3-540-28333-1). URL: <https://cds.cern.ch/record/976471>.
- [13] Tai Sakuma. ‘Cutaway diagrams of CMS detector’. In: (May 2019). URL: <https://cds.cern.ch/record/2665537>.
- [14] *Silicon Pixels Sensors at CMS*. URL: <https://home.cern/science/accelerators/large-hadron-collider>.
- [15] *The High-Luminosity large Hadron Collider*. URL: <https://home.cern/resources/faqs/high-luminosity-lhc>.
- [16] *The Large Hadron Collider*. URL: <https://home.cern/science/accelerators/large-hadron-collider>.
- [17] V A.J Van Lint et al. ‘Mechanisms of radiation effects in electronic materials. Vol. 1’. In: (Jan. 1980). URL: <https://www.osti.gov/biblio/6854931>.
- [18] Pascal Vanlaer et al. ‘The Phase-2 Upgrade of the CMS Tracker’. In: 2017.
- [19] L. Wiik-Fuchs et al. ‘Annealing studies of irradiated p-type sensors designed for the upgrade of ATLAS phase-II strip tracker’. In: *Nuclear Instruments and Methods in Physics Research Section A: Accelerators, Spectrometers, Detectors and Associated Equipment* 924 (2019). 11th International Hiroshima Symposium on Development and Application of Semiconductor Tracking Detectors, pp. 128–132. ISSN: 0168-9002. DOI: <https://doi.org/10.1016/j.nima.2018.10.014>. URL: <https://www.sciencedirect.com/science/article/pii/S0168900218313299>.

- [20] Renate Wunstorf. ‘Systematische Untersuchungen zur Strahlenresistenz von Silizium-Detektoren für die Verwendung in Hochenergiephysik-Experimenten’. University of Hamburg, Diss., 1992. Dr. Hamburg: University of Hamburg, 1992. URL: <https://bib-pubdb1.desy.de/record/153817>.

Appendix A

Code and Data Location

1. GitHub CMS Folder:

https://github.com/AndrewTKent/CERN_CMS_Silicon_Sensor

2. Annealing Temperature Conversion:

https://github.com/AndrewTKent/CERN_CMS_Silicon_Sensor/tree/main/Diodes/DZero/Annealing_Conversion

3. HGCAL Hamburg Analysis:

https://github.com/AndrewTKent/CERN_CMS_Silicon_Sensor/tree/main/Diodes/HGCAL/Hamburg_Analysis

4. Alibava Annealing Studies:

https://github.com/AndrewTKent/CERN_CMS_Silicon_Sensor/tree/main/Diodes/Halfmoon/Annealing

5. Ljubljana vs. Rinsc Analysis:

https://github.com/AndrewTKent/CERN_CMS_Silicon_Sensor/tree/main/Diodes/Ljubljana_Diodes

6. Pin Diodes:

https://github.com/AndrewTKent/CERN_CMS_Silicon_Sensor/tree/main/Diodes/Pins